REVIEWS

Reactor Modeling for Polymerization Processes

Carlos M. Villa*

The Dow Chemical Company, Freeport, Texas 77541

The engineering principles that apply to polymerization reactions are extensions of well-established principles for the study of reactions that involve small molecules. Macromolecules are very attractive, because, through changes in their molecular architecture, one can influence end-use properties that small molecules do not have, such as melt strength, crystallinity, and clarity, to name a few. This additional degree of freedom comes at a cost, however, because it introduces a level of complexity that requires careful consideration during reactor design, analysis, and/or operation. There are many practical problems in polymer reaction engineering that can be handled using traditional tools. Very little additional expertise is required from reaction engineers. There are other problems that demand this expertise and, because they do, it becomes more difficult to avoid empirical components and determine when an observation should be predicted by the model or handled as a measurement artifact. This review attempts to define the borders that separate these two types of problems and discusses the challenges and opportunities industry often faces. There are still practical problems to solve in the area of commodity polymers, and there are many opportunities to apply the same engineering principles to specialty polymers.

Introduction

The polymer industry consumes more than half of the tonnage output of the organic chemical industry,[1] and only a few polymers dominate this industry. Transition-metal catalysts are used to produce polypropylene, high-density polyethylene (HDPE), and linear low-density polyethylene (LLDPE), whose combined output was responsible for 42% of the 41 million metric tons of thermoplastic resins produced in the United States in the year 2000. Another 40% represented a handful of polymers that are produced using the free-radical mechanism: low-density polyethylene (LDPE), poly(vinyl chloride) (PVC), polystyrene, poly(vinyl alcohol) (PVA), poly(methyl methacrylate) (PMMA), and poly(vinyl acetate). Most of the remaining 18% corresponds to polyurethanes and a few condensation polymers, such as polyethylene terephtalate, polybutylene terephtalate, polyamides, and polycarbonates. Even the period from 2000 to 2005, which was one of significant stress and change for the U.S. chemical industry,[2] was not enough to force a dramatic change in the landscape, as illustrated by Figure 1.

The dominant polymers are old polymers, and their current market share is not very different from what it was decades ago. They have not been replaced by new materials, because their volumes encourage both producers and consumers to develop incremental improvements in properties and manufacturing techniques, rather than overnight replacements with materials that have novel properties. This may initially seem like the description of an industry where little change occurs over time; however, the polymer industry is anything but that. Polymer producers are faced with many challenges, and they must adjust to those challenges or perish. The obvious—and, perhaps, more important—challenge is their strong dependence on natural gas and oil, both as energy sources and as sources of raw materials. This creates a dynamic environment where
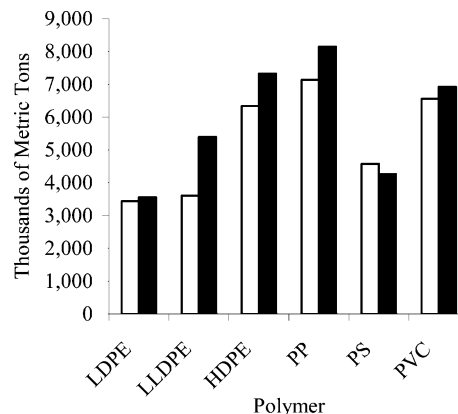

Figure 1. Bar graph showing the U.S. polymer industry in the United States (□) in 2000 and (■) in 2005.

polymers and their manufacturing processes undergo continuous improvement in an effort to keep existing markets and to penetrate the markets of other materials, polymers or not. Thus, the polymer industry is concerned with research and development efforts in at least the following areas:

(1) improved understanding of polymerization processes and their effect on product performance;

(2) traditional polymers with improved properties;

(3) more-efficient process technology;

(4) new polymers; and

(5) renewable sources of raw materials

We will examine examples of efforts in some of these areas. Many disciplines are involved in those efforts; however, we will be concerned mainly with the reaction schemes at work in polymerization processes and their impact on product properties.
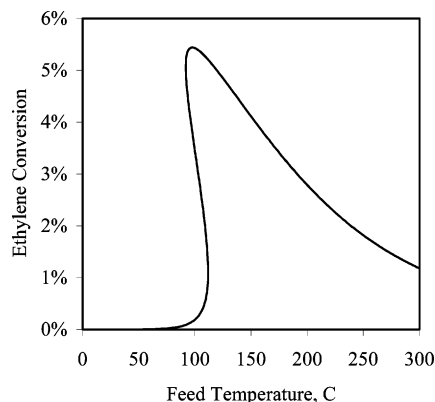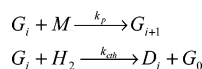
* E-mail address: cmvilla@dow.com.

Figure 2. Plot showing ethylene conversion in an autoclave low-density polyethylene (LDPE) reactor.

Scheme 1. Propylene Polymerization

$$G_i + M \xrightarrow{k_p} G_{i+1}$$
$$G_i + H_2 \xrightarrow{k_{ch}} D_i + G_0$$

Improved Understanding of Polymerization Processes and Their Effect on Product Performance

The behavior of a polymerization reactor is not different from the behavior of any other reactor, so the same engineering principles apply in both cases. Most polymerization reactions are strongly exothermic, which demands reactor configurations with adequate rates of heat removal. This means also that interesting dynamic behavior is possible, under certain conditions. Figure 2 illustrates this observation for an autoclave reactor used in LDPE production. This is an adiabatic reactor operating at feed temperatures that are low enough to maximize conversion and avoid an explosive runaway due to ethylene decomposition, but are not so low that the risk of reaction extinction is high.[3] There are many complications to consider in regard to searching for the optimum set of conditions of any exothermic reactor. Polymerization reactors make the search more difficult, because one must also consider the effect that those conditions will have on product properties. Propylene polymerization reactors provide a simple illustration of the challenges one faces in choosing the right operating conditions for the desired product.

Polypropylene is normally made using heterogeneous catalysts in liquid or gas-phase reactors. A typical fourth-generation Ziegler–Natta catalyst for propylene polymerization can easily reach a mileage of 30–80 kg polymer/g catalyst.[4] The reaction scheme can be complex, but two reactions influence reactor performance and polymer properties the most. Using G_i to represent growing chains of length i, D_i to represent dead chains of length i, M to represent monomer, and H_2 to represent hydrogen, the two reactions are described by Scheme 1.

Monomer consumption happens during chain growth, and one needs a rate expression for this step to be able to describe the effect that temperature, catalyst feed rate, and other conditions have on mass and energy balances. The rate expression corresponding to the chain growth reaction in Scheme 1 is

$$R_p = k_p M G \tag{1}$$

where G, which represents the total concentration of polymer chains (or active catalytic sites), is defined as

$$G = \sum_{i=0}^{\infty} G_i \tag{2}$$

Upon closer inspection, however, our conception of catalyst activity turns out to be slightly more complex. Propylene insertion can occur two ways: 1–2 (primary) and 2–1 (secondary), leading to the four alternate scenarios shown in Figure 3.

The 2–1 insertions are believed to slow propagation by forming dormant sites that become active again after a 1–2 insertion or a chain-transfer reaction.[5] The entire process can be described now using P and S to represent active and dormant sites, respectively (see Scheme 2).

Assuming the quasi-steady-state approximation, the exchange from dormant to active sites satisfies the relation

$$k_{ps} P M = k_{sp} S M + k_{sH} S \sqrt{[H_2]} \tag{3}$$

The square-root dependency of the rate of chain transfer on hydrogen concentration ($[H_2]$) was reported by Natta and co-workers more than 50 years ago,[6] and it remains largely unchallenged. In terms of all active sites, $G = P + S$, the rate of polymerization is finally expressed as

$$R_p \approx \frac{k_{sp} M + k_{sH} \sqrt{[H_2]}}{k_{ps} M + k_{sp} M + k_{sH} \sqrt{[H_2]}} k_{pp} M G \tag{4}$$

Thus, catalyst activity is higher in the presence of hydrogen than in its absence; this is an activating effect that is well-known for fourth-generation Ziegler–Natta catalysts used in propylene polymerization. The new expression for the polymerization rate should provide a more accurate picture of catalyst activity, but activity is not our only concern. Average chain lengths are very important because they determine the application that a polypropylene resin is intended for. Assuming that the observed number average chain length is mainly determined by the polymer growing at the active sites:

$$X_n \approx \frac{k_{pp} M}{k_{pH} \sqrt{[H_2]}} \tag{5}$$

In the case of polypropylene, there is an end-use property that identifies, better than anything else, the type of resin that one is after. This is the melt flow rate (MFR), which is normally correlated with the weight-average molecular weight (M_w):[7]

$$\text{MFR} = a_1 M_w^{a_2} \tag{6}$$

It is not surprising to see an almost-linear dependence of MFR on the hydrogen concentration on a log–log plot, such as that shown in Figure 4, especially at medium and high hydrogen concentrations. When the concentration of hydrogen is low, the curve changes slope, because other chain termination mechanisms become dominant. Coefficient a_2 is normally close to 4; therefore, given the square-root dependency of the rate of chain transfer on hydrogen concentration, we should expect a slope of ~2. Thus, the slope of the line is fixed, but its location shifts, because the hydrogen response varies from catalyst to catalyst. Implicit in this derivation is the assumption that the ratio of number-average and weight-average chain lengths is fixed, which seems to be a reasonable assumption for many fourth-generation Ziegler–Natta catalysts.
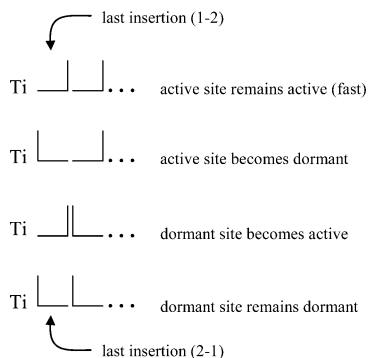
Figure 3. Propylene insertion during polymerization.

Scheme 2.   Primary and Secondary Propylene Insertion

$$P + M \xrightarrow{k_{pp}} P$$
$$P + M \xrightarrow{k_{ps}} S$$
$$S + M \xrightarrow{k_{sp}} P$$
$$S + M \xrightarrow{k_{ss}} S$$
$$P + H_2 \xrightarrow{k_{pH}} D + P$$
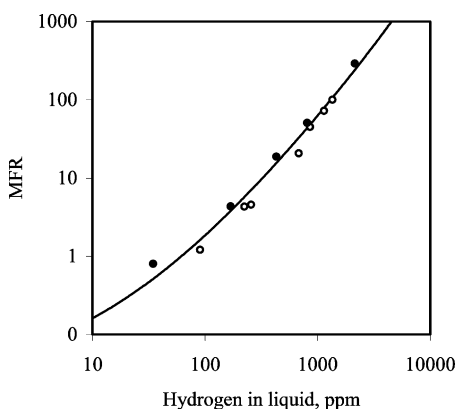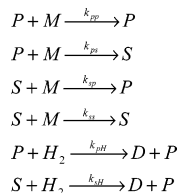$$S + H_2 \xrightarrow{k_{sH}} D + P$$

Figure 4. Effect of hydrogen on the melt flow rate (MFR) of polypropylene produced in (—) a batch laboratory reactor, (●) a continuous miniplant reactor, and (○) a continuous pilot-plant reactor.

Figure 4 shows good agreement for the chosen catalyst as the reactor type and scale are modified.[8] The line represents a model prediction developed using data from a laboratory reactor that produced polymer samples with medium and low MFR values. The model has been extrapolated to high MFR values, and it agrees well with data from a miniplant and a pilot plant. Figure 4 illustrates the modern trend toward answering most scale-up questions in small reactors before moving to reactors more similar to the size found in production plants.[9]

The picture is of course more complex than it seems at first sight. Hydrogen is present in very low concentrations, and it is a real challenge both to measure it and to predict its concentration for a given set of operating conditions. Another problem that is encountered with models of propylene polymerization reactors is that the concentrations needed to use in the kinetic mechanism should be the concentrations near the active sites, and these are rarely known. One is usually forced to use bulk concentrations, because little is known, for example, about the solubility of hydrogen in the polymer phase that surrounds the catalyst. This represents a serious problem when kinetic measurements are available for a catalyst in a liquid-phase reactor, and it is desired to extend the model to gas-phase reactors. The available evidence indicates that the same kinetic mechanism can be used in liquid- and gas-phase reactors; however, that evidence is unfortunately scarce.[10]
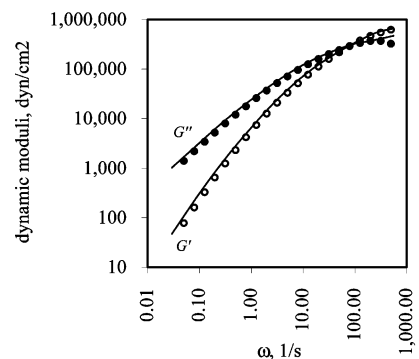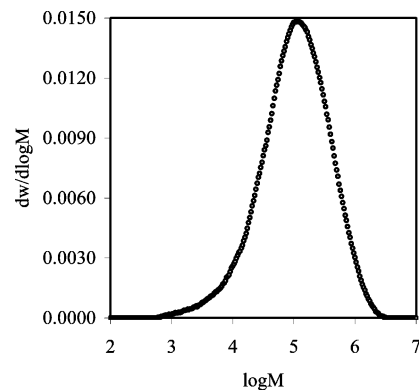

Figure 5. Measured and predicted dynamic moduli corresponding to the observed molecular weight distribution.

Despite all these difficulties, there is still much that one can predict by relying on a simple polymerization scheme. The scheme should lead, for example, to the molecular weight distribution of the polymer. With $w(M)$ dM as the weight fraction of chains that have molecular weights between M and $M + $ dM, the relaxation spectrum of the polymer can be computed as[11]

$$\tilde{h}(M) = \frac{\beta G_N^0}{\alpha} w(M) \left[\int_M^\infty w(s) \frac{\mathrm{d}s}{s} \right]^{\beta - 1} \tag{7}$$

The relaxation spectrum allows calculation of many rheological properties, such as the dynamic moduli:

$$G'(\omega) = \int_0^\infty h(\tau) \frac{(\omega\tau)^2}{1 + (\omega\tau)^2} \frac{\mathrm{d}\tau}{\tau} \tag{8}$$

$$G''(\omega) = \int_0^\infty h(\tau) \frac{\omega\tau}{1 + (\omega\tau)^2} \frac{\mathrm{d}\tau}{\tau} \tag{9}$$

In addition to the molecular weight distribution, the model requires values of three parameters: G_N^0, β, and α. These are already available for linear polymers such as polypropylene or polystyrene. Figure 5 illustrates the application of this technique to a sample of polypropylene.

An improved understanding of the polymerization processes and their effect on product performance is necessary to be able to make those processes as efficient as possible. The models that summarize that understanding are not required to be complex, and it is already possible to generate a siginificant fraction of the necessary knowledge in systems that are much smaller than the world-scale plants, where polymers are typically produced. However, important gaps still remain in our knowledge and these must be addressed. Polypropylene is one of the simplest, better understood polymers, because it is a linear molecule. It quickly becomes difficult to evaluate very quickly
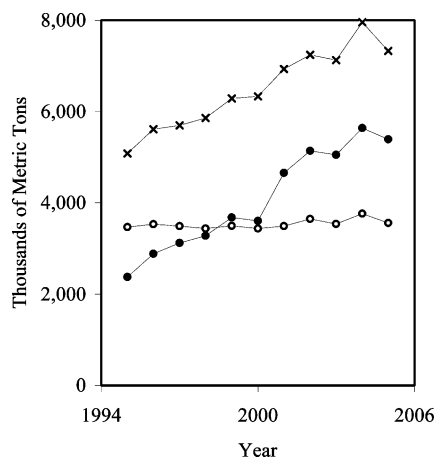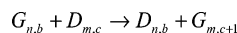
Figure 6. Graph showing the activity of the polyethylene market in the United States over the last 10 years: (○) LDPE, (●) LLDPE, and (×) HDPE.

Scheme 3. Transfer to Polymer in Free-Radical Ethylene Polymerization

$$G_{n,b} + D_{m,c} \rightarrow D_{n,b} + G_{m,c+1}$$

when one considers polymers with more-complex molecular architecture, such as branched polyethylene.

Traditional Polymers with Improved Properties

Figure 6 shows how the polyethylene market in the United States has evolved recently toward an increasing market share for HDPE and LLDPE at the expense of LDPE.[2] The incentive to build plants for the production of LDPE is not great enough, because of the extreme operating conditions involved. However, LDPE remains an attractive product; it is attractive enough to keep the current plants operating. HDPE is produced under less-demanding conditions than LDPE; however, being a linear molecule, it is not able to drive LDPE out of the market. Co-monomers such as 1-octene add short branches to HDPE, leading to a reduction in its crystallinity and its density, which makes it more similar to LDPE. The resulting LLDPE has more regular branching than LDPE, and this translates to better tensile strength. Unfortunately, 1-octene is more expensive than ethylene. This explains the constant search for catalyst families that are capable of producing polyethylene resins with equal or better properties than the current alternatives, but at lower costs.

LDPE is the polymer that comes to mind when branching is mentioned, and chain transfer to the polymer provides the route to branching. In this route, a growing molecule that contains n repeating units and b branches abstracts a H atom from a dead chain that contains m repeating units and c branches (see Scheme 3). The two molecules switch roles, from growing to dead and vice versa, and the number of branches in the new growing molecule increases by 1. This happens because hydrogen abstraction from a dead molecule can happen anywhere, not just at the ends, and monomer addition is so fast that the new growing molecule is very likely to end up with one more branching point, as illustrated in Figure 7.

The degree of branching of LDPE is often estimated by comparing the intrinsic viscosity of the branched material to the intrinsic viscosity of linear polyethylene of the same molecular weight. The ratio of the two viscosities is used to compute the mean-square radii of gyration:[12]

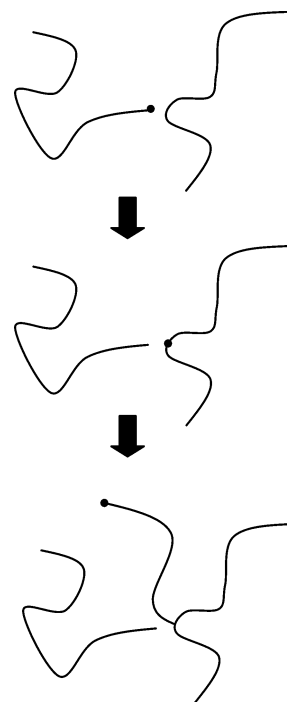$$g^2 = \frac{[\eta]_{branched}}{[\eta]_{linear}} \tag{10}$$

Figure 7. Schematic depiction of long-chain branching in LDPE.

The equation that relates g to the number of trifunctional branch points (m) was derived by Zimm and Stockmayer:[13]

$$g = \left(\sqrt{1 + \frac{m}{6}} + \frac{4m}{3\pi} \right)^{-1/2} \tag{11}$$

The number of trifunctional branch points, on the other hand, can be expressed in terms of process conditions and kinetic parameters. The rate of the chain-transfer reaction that generates those points is[14]

$$R_{LCB} = k_{LCB} \sum_{n=1}^{\infty} \sum_{b=1}^{\infty} G_{n,b} \sum_{m=2}^{\infty} \sum_{c=1}^{\infty} m D_{m,c} \tag{12}$$

In this rate expression, the first factor is the total concentration of growing chains and the second factor is the concentration of repeating units in dead chains. The rate is proportional to the concentration of repeating units, rather than the concentration of dead chains, because all the C atoms along a dead chain should be available for attack. This assumption, by the way, is not universally accepted.[15] In an autoclave reactor, for instance, the rate expression for R_{LCB} leads to the following measure for the number of long-chain branches per 1000 C atoms:

$$LCB = 500 \tau k_{LCB} \sqrt{\frac{2 f k_d I}{k_t}} \tag{13}$$

The process model is simple and the technique used to estimate the degree of branching also is simple; however, one must be prepared to accept the limitations of this scheme. Estimates of LCB are usually obtained by gel permeation chromatography (GPC), so they have the potential to drift as new separation columns are introduced. Also, the conditions in some reactor configurations may be such that the theory developed by Zimm and Stockmayer is not exactly applicable. Ultimately, this approach to measuring the degree of branching generates less-than-ideal (and possibly drifting) estimates of k_{LCB}. In such cases, one is faced with a common dilemma:
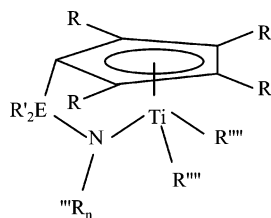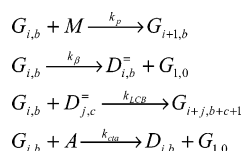
Figure 8. Schematic depiction of the structure of a constrained geometry catalyst (CGC) procatalyst.

Scheme 4. Long-Chain Branching in Constrained Geometry Catalysts (CGCs)

$$G_{i,b} + M \xrightarrow{k_p} G_{i+1,b}$$
$$G_{i,b} \xrightarrow{k_\beta} D_{i,b}^= + G_{1,0}$$
$$G_{i,b} + D_{j,c}^= \xrightarrow{k_{LCB}} G_{i+j,b+c+1}$$
$$G_{i,b} + A \xrightarrow{k_{cta}} D_{i,b} + G_{1,0}$$

develop a more reliable but elaborate scheme for estimating k_{LCB}, or continue to use the less reliable and simpler scheme but be able to apply it everywhere.

Branching is not a property that is possessed only by LDPE, and significant efforts have gone into developing catalyst families that can introduce branching in systems where transfer to polymer is absent. One of those is the family of constrained geometry catalysts (CGCs). These catalysts have mileages in excess of 5000−7000 kg polymer/g metal, at temperatures as high as 180 °C, with molecular weights that are similar to those obtained from traditional Ziegler−Natta catalysts, and with better α-olefin incorporation levels.[16] A well-studied CGC procatalyst is illustrated in Figure 8. This is normally activated with mixtures of modified methylalumoxane (MMAO) and *tris*-perfluorophenylborane (FAB).

Long-chain branching during ethylene polymerization with CGCs has been atributed to β-hydride elimination.[17] This step forms an unsaturated dead polymer chain that is capable of being inserted into a growing polymer chain in a step that is analogous to the usual insertion of a monomer molecule. With M and A representing the monomer and the chain-transfer agent, the reaction scheme is given in Scheme 4. $G_{i,b}$ and $D_{i,b}$ correspond in this case to growing and dead chains with i repeating units and b branches. Unsaturated dead chains are represented by $D_{i,b}^=$.

In a continuously stirred tank reactor (CSTR) at steady state, with τ representing the average residence time of the reactor, this mechanism leads to the following population balance for dead chains:

$$0 = -D_{i,b} + \tau k_{cta} A G_{i,b} \tag{14}$$

The population balance for unsaturated dead chains is

$$0 = -D_{i,b}^= + \tau k_\beta G_{i,b} - \tau k_{LCB} D_{i,b}^= \sum_{j=1}^{\infty} \sum_{c=0}^{\infty} G_{j,c} \tag{15}$$

The population balance for growing chains of length zero is

$$0 = G_{1,0}^f - G_{1,0} + \tau(k_\beta +$$
$$k_{cta} A) \sum_{j=1}^{\infty} \sum_{c=0}^{\infty} G_{j,c} - \tau k_p M G_{1,0} - \tau k_{LCB} G_{1,0} \sum_{i=1}^{\infty} \sum_{b=0}^{\infty} D_{i,b}^= \tag{16}$$

Finally, the population balance for growing chains of a length greater than zero is

$$0 = -G_{i,b} - \tau(k_\beta + k_{cta} A + k_{LCB} \sum_{j=1}^{\infty} \sum_{c=0}^{\infty} D_{j,c}^=)G_{i,b} - \tau k_p M$$
$$(G_{i,b} - G_{i-1,b}) + \tau k_{LCB} \sum_{j=1}^{\infty} \sum_{c=0}^{\infty} G_{i-j,c} D_{j,b-c-1}^= \tag{17}$$

Soares and Hamielec showed that the bivariate distribution of chain lengths and the number of chain branches corresponding to these polymer populations is[17]

$$f_{i,b} = \frac{1}{(2b)!} i^{2b} p^{2b+1} e^{-pi} \tag{18}$$

where p is a ratio of reaction rates:

$$p = \frac{R_\beta + R_{ct} + R_{LCB}}{R_p} \tag{19}$$

This case shows well how a reaction scheme can be turned into a description of the molecular architecture of a polymer and how quickly that description becomes very complex. It also serves as a reminder that model development does not end, but merely begins, at the point where one finds an expression relating process conditions to molecular architecture. Two significant challenges are usually met. One of them is the need to calibrate and validate such a model. The other challenge is to link a molecular architecture model with a product performance model. The product performance model is usually a set of empirical correlations that relate the properties that users care about (such as melt strength, crystallinity, and clarity: the so-called end-use properties) with properties that users do not often care about (such as the degree of branching, the number-average molecular weight, and the polydispersity index).

More-Efficient Process Technology

The development of new polymeric materials that can self-assemble requires precise control over the molecular architecture of those materials. For this purpose, the ideal polymerization mechanism is one that provides the degree of control typical of biological systems. The next-best option is provided perhaps by living polymerization,[18] which is described as a chain polymerization from which irreversible chain transfer and irreversible chain termination are absent.[19]

With M representing monomer and G_i the growing chains, a reaction scheme that describes living polymerization can be represented as shown in Scheme 5.

Similar to the simple scheme that transforms A to B and B to C, the living polymerization scheme leads to a distribution of products, rather than the single product that biological systems are capable of producing. However, the distribution can be very narrow.

Living polymerization is not considered to be useful, simply because of its potential contribution to the development of materials that can self-assemble. It already has an application in the manufacture of block copolymers (a good example is the styrene−butadiene block copolymer[20]). Unfortunately, the number of applications of living polymerization and the volume of those applications remain low, despite all the excitement generated recently by living free-radical polymerization. One would not expect to hear of a class of polymers produced through what seems to be a living polymerization mechanism by consuming a significant portion of one of the top-50 highest-volume chemicals in the United States.[1] But there is such a class. These polymers are known as polyether polyols, and they
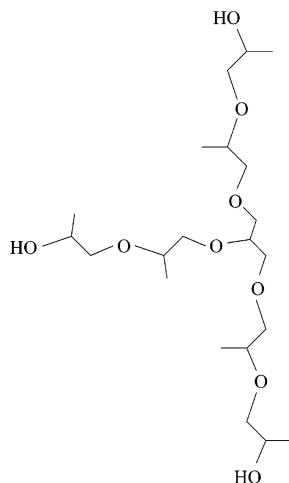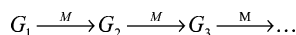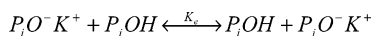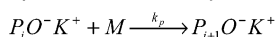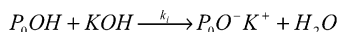
Figure 9. Schematic depiction of the structure of a glycerine-initiated polyether polyol.

Scheme 5. Living Polymerization

$$G_1 \xrightarrow{M} G_2 \xrightarrow{M} G_3 \xrightarrow{M} \ldots$$

Scheme 6. Propylene Oxide Polymerization

$$P_0OH + KOH \xrightarrow{k_i} P_0O^-K^+ + H_2O$$

$$P_iO^-K^+ + M \xrightarrow{k_p} P_{i+1}O^-K^+$$

$$P_iO^-K^+ + P_jOH \xleftarrow{K_e} P_iOH + P_jO^-K^+$$

consumed almost two-thirds of the 1.8 million metric tons of propylene oxide produced in the United States in the year 2000. They also consumed a smaller, but significant, portion of the 3.9 million metric tons of ethylene oxide produced in the same year.

In 1940, Flory assumed that ethylene oxide polymers would be produced by a living polymerization mechanism.[21] However, in propylene oxide polymers, there is a chain-transfer reaction that is responsible for the continuous generation of a minor population of unsaturated monofunctional chains that makes it difficult to reach long chain lengths. This chain-transfer reaction does not lead to irreversible termination of the dominant polyol chains, as expected for a living polymerization scheme, but it does add new chains continuously.

Commercial polyols typically have chain lengths of ≤100, and they find their main application in the production of polyurethanes. Polyurethanes have a wide variety of applications, and they owe a great deal of this flexibility to the polyols used in their manufacture. Depending on the application for which the polyurethane is intended, the polyol can be a polyether or a polyester, with primary or secondary hydroxyl groups, with high or low functionality, and with long or short chains.[22]

One can make a propoxylated triol, for example, using a molecule of glycerine as the starting point. Open-ring polymerization of propylene oxide will generate a polyol molecule with terminal secondary hydroxyl groups attached to polyether backbones, as shown in Figure 9. The longer these backbones, the more flexible the polyurethane foam.

The catalyst of choice in the ring-opening polymerization of polyethers such as ethylene oxide and propylene oxide is potassium hydroxide (KOH), and, ignoring the effect of the chain-transfer reaction that produces unsaturated monofunctional chains, three reaction steps are sufficient for a reasonable description of chain development: initiation, growth, and exchange. (See Scheme 6.) The initiator is converted to an active alkoxide ion in the first reaction. In the second reaction, a
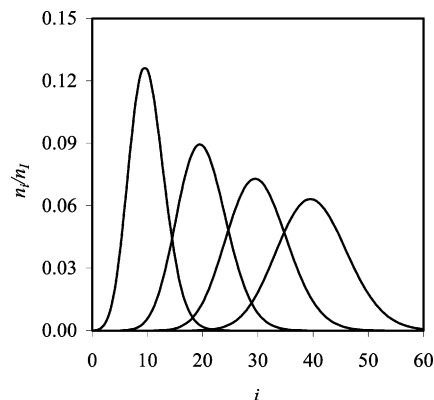

Figure 10. Poisson distributions for number-average chain lengths of X_n = 10, 20, 30, and 40.

growing alkoxide ion of length i adds one monomer unit to become an ion of length $i + 1$. The third reaction describes the fast exchange between dormant (alcohol) and growing (alkoxide) end groups. The number of polyol chains is normally greater than the number of K^+ ions; however, the fast exchange gives every chain the chance to grow to almost the same length.[23]

In an isothermal semibatch reactor with a continuous addition of monomer, the population balance for polymer species has the following form:

$$\frac{dn_0}{dt} = -\kappa n_0 \quad (20)$$

$$\frac{dn_i}{dt} = \kappa n_{i-1} - \kappa n_i \quad \text{(for } i > 0\text{)} \quad (21)$$

where n_i represents the number of moles of chains of length i, t is the time, and κ is a reaction coefficient that we will revisit later. When the initiator is a monodisperse substance, and n_I represents the number of moles of this initiator, the equations should be integrated with the following initial conditions: $n_0 = n_I$ and $n_i = 0$ for $i > 0$. The solution is

$$\frac{n_i}{n_I} = \frac{(\kappa t)^i}{i!} e^{-\kappa t} \quad (22)$$

The number chain-length distribution that corresponds to these properties is the Poisson distribution, shown in Figure 10 for number-average chain lengths of 10, 20, 30, and 40. This length is given by

$$X_n = \kappa t \quad (23)$$

Other properties of interest include the weight-average chain length (X_w) and the polydispersity index (PDI):

$$X_w = 1 + \kappa t \quad (24)$$

$$\text{PDI} = 1 + \frac{1}{\kappa t} \quad (25)$$

In an isothermal CSTR at steady state, when a monodisperse initiator is fed into the reactor and τ is used to represent the average residence time of that reactor, the population balance for polymer species has the following form:

$$0 = n_I - n_0 - \tau \kappa n_0 \quad (26)$$

$$0 = -n_i + \tau \kappa n_{i-1} - \tau \kappa n_i \quad \text{(for } i > 0\text{)} \quad (27)$$
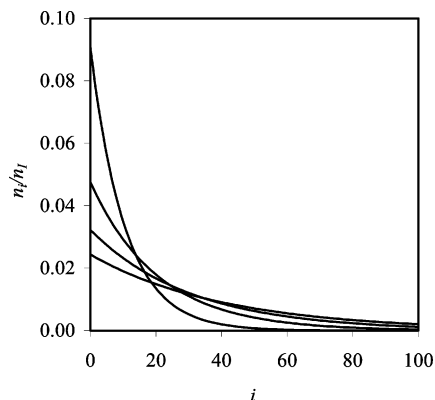
Figure 11. Most-probable distributions for number-average chain lengths of $X_n = 10, 20, 30,$ and 40.

The solution to the new system of equations is

$$\frac{n_i}{n_I} = \frac{1}{1 + \tau\kappa}\left[\frac{\tau\kappa}{1 + \tau\kappa}\right]^i \qquad (28)$$

The properties that characterize this solution are

$$X_n = \tau\kappa \qquad (29)$$

$$X_w = 1 + 2\left(\frac{(\tau\kappa)^2}{1 + \tau\kappa}\right) \qquad (30)$$

$$\mathrm{PDI} = \frac{1}{\tau\kappa} + 2\left(\frac{\tau\kappa}{1 + \tau\kappa}\right) \qquad (31)$$

The number chain-length distribution that corresponds to this solution is the most probable distribution, and it is shown in Figure 11 for number-average chain lengths of 10, 20, 30, and 40.

Figures 10 and 11 clearly illustrate the dramatic impact that reactor configuration has on polymer properties. This fact has been known for many years,[24] and we have discussed it in detail only because it provides a good introduction to the current state of affairs in polyol manufacture.

The manufacture of polyols is now experiencing a dramatic transformation that is, in some ways, similar to the transformation that the polyolefins industry experienced decades ago.[25] Common catalysts such as KOH are being replaced by a family of very active catalysts that can be used in low concentrations. Separation from the final product is avoided. This is the family of double-metal cyanide (DMC) catalysts, which is represented, for example, in a recent patent by[26]

$$M^1_x([M^2_{x'}(\mathrm{CN})_y]_z\cdot[M^3_{-x-}\mathrm{A}_{-y-}]\mathrm{L}^1\cdot\mathrm{L}^2\cdot M^4\mathrm{B}_z)$$
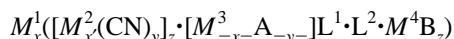
where M^1 is a metal, $M^2_{x'}(\mathrm{CN})_y$ a metal cyanide, $M^3_{-x-}\mathrm{A}_{-y-}$ a transition-metal salt, $M^4\mathrm{B}_z$ an alkali-metal salt, L^1 an organic complexing ligand, and L^2 a functionalized polymer.

A common formulation uses zinc as M^1, $\mathrm{Co(CN)}_6$ as $M^2_{x'}\mathrm{CN}_y$, ZnCl_2 as $M^3_{-x-}\mathrm{A}_{-y-}$, and t-BuOH as L^1. Much remains to be known about the way these catalysts work and about the role that each of its components has in the process. In the meantime, they are generating surprising results, such as that shown in Figure 12. The molecular weight distributions of polyols produced in CSTRs, using DMC catalysts, are more similar to the molecular weight distributions of polyols produced in semibatch reactors using KOH as a catalyst. Their polydispersities do not approach the expected value of 2, but are usually low.[27] This unusual behavior has been attributed to "differential
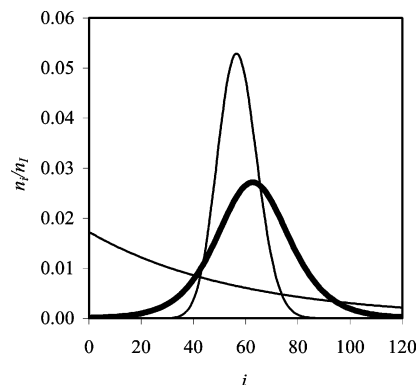

Figure 12. Number-average chain-length (X_n) distributions of polyols prepared using potassium hydroxide (KOH) in semibatch and continuous reactors (thin lines) and double-metal cyanide (DMC) in continuous reactors (thick line).

catalytic activity" that favors the growth of short chains over the growth of long chains.

To understand the source of the differential catalytic activity of DMC catalysts, it is convenient to take a closer look at the reaction coefficient κ. Assuming that the exchange step has a similar role in both KOH and DMC catalysis, it is possible to arrive at the following expression for κ:

$$\kappa = \frac{k_p M}{1 + K_e[(n_I - n_C)/n_C]} \qquad (32)$$

The differential activity of DMC catalysis could be caused by a decrease in the rate coefficient for chain growth, an increase in the rate coefficient for transformation of growing species into dormant ones, and/or a decrease in the rate coefficient for transformation of dormant species into growing ones, as the chain length increases. The values of the propagation rate coefficients decrease as the chain length increases in some free-radical polymerization systems, and the variation is more dramatic at chain lengths of 200 or less.[28] Regardless of the mechanism, this behavior has a significant effect over the reactor configurations that one is allowed to use and the types of products one is allowed to produce. This behavior also raises a few questions, such as

(1) Is the differential catalytic activity restricted to DMC, or is it a consequence of the heterogeneous nature of these catalysts?

(2) Could the differential catalytic activity be extended to other living polymerization systems that would benefit from continuous operation?

New Polymers and Renewable Sources of Raw Materials

Polyols also illustrate the challenges associated with the search for new polymers and new sources of raw materials. In this case, the new polymers are hyperbranched polyols, which are obtained via the ring-opening polymerization of glycidol.[29] With glycerine as an initiator, the reaction with 10 molecules of glycidol gives many possible isomers, one of those being that shown in Figure 13. Because glycidol can be obtained from glycerol, this system also fits well with the recent trend to produce polymers from biorenewable materials.

When glycidol adds to a secondary alcohol group in the polyol molecule, a new secondary alcohol group and a new primary alcohol group are formed. When glycidol adds to a primary alcohol group in the polyol molecule, a new secondary alcohol group and a new primary alcohol group are formed. The first
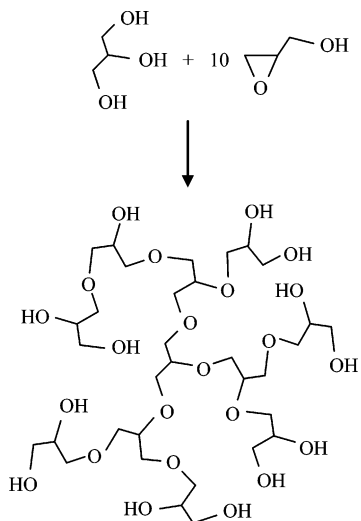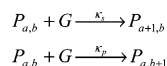
Figure 13. Schematic depiction of the open-ring polymerization of glycidol to produce hyperbranched polyols.

Scheme 7. Glycidol Addition to Glycerine

$$P_{a,b} + G \xrightarrow{\kappa_s} P_{a+1,b}$$
$$P_{a,b} + G \xrightarrow{\kappa_p} P_{a,b+1}$$

addition increases the net number of primary alcohol groups by one, whereas the second addition increases the net number of secondary groups by one. Thus, if G represents glycidol, $P_{a,b}$ represents a polymer molecule with a primary and b secondary alcohol groups, κ_p represents the rate coefficient for addition to primary, and κ_s represents the reaction coefficient for addition to secondary, this process could be represented by Scheme 7. The scheme is reminiscent of the living polymerization mechanism described previously. It provides the means to determine the distribution of the number of primary alcohol groups, the distribution of the number of secondary alcohol groups, and the distribution of the number of repeating units, which is given by

$$n = a + b - 2 \qquad (33)$$

As noted previously, a hyperbranched polyol such as that shown in Figure 13 is not the only possible isomer formed by the open-ring polymerization of glycidol. The number of repeating units added to glycerine is not just 10 either. This is a departure from what one is used to seeing in traditional polyols, where the number of alcohol groups per molecule is always the same (3 in triols or 2 in diols, for example). Instead of a fixed number of alcohol groups, one gets a distribution of numbers in hyperbranched polyols. The importance of this difference really is dependent on the behavior of the polyol when it forms the polyurethane foam and, later, on the performane of that foam. This brings us back to what we observed early on, which is the problem of relating process conditions to product performance, except the product whose molecular architecture with which we are now concerned—the polyol—is not the end point, but, rather, only an intermediate.

Conclusions

Our ability to improve the efficiency of polymerization processes and the properties of the polymers they produce is associated with our understanding of those processes. This understanding is usually condensed in the form of a molecular architecture model that corresponds to a reactor design and the way that reactor is operated. Unfortunately, a molecular architecture model alone does not provide the language that allows communication between the producer and the consumer. That language also requires a model of product performance to allow the transition from the producer to the consumer.

New catalysts and new sources of monomeric raw materials are not likely to transform the polymer industry overnight. However, despite the firm grip of traditional materials, there is still plenty of room for new developments, as evidenced by the discovery of new transition-metal catalysts and the gradual increase in market share of polymers manufactured using these catalysts. Reaction engineers have an important role in these developments, because they have the ability to describe the type of molecular architecture that a new reaction mechanism is capable of producing and to use this information to help guide the process of discovering new catalysts and the materials generated by those catalysts.

Nomenclature

A = chain-transfer agent

D_i = linear dead chain with i repeating units

$D_{i,b}$ = branched dead chain with i repeating units and b branches

$D_{i,b}^=$ = branched unsaturated dead chain with i repeating units and b branches

f = initiator efficiency

$f_{i,b}$ = fraction of chains with i repeating units and b branches

g^2 = mean-square radii of gyration

G = glycidol

G_N^0 = plateau modulus

G_i = linear growing chain with i repeating units

$G_{i,b}$ = branched growing chain with i repeating units and b branches

$[H_2]$ = concentration of hydrogen

I = initiator

k_d = rate coefficient for initiator decomposition

k_{cta} = rate coefficient for chain transfer to agent

k_{cth} = rate coefficient for chain transfer to hydrogen

k_{LCB} = rate coefficient for long-chain branching

k_p = rate coefficient for chain growth

k_β = rate coefficient for β-hydride elimination

K_e = equilibrium constant of exchange (active to dormant) reaction

M = monomer

M = molecular weight

M_n = number-average molecular weight

M_w = weight-average molecular weight

MFR = melt flow rate

n_C = moles of alkoxylation catalyst

n_i = moles of polyol chain with i repeating units

n_I = moles of initiator

$P_{a,b}$ = hyperbranched polyol molecule with a primary alcohols and b secondary alcohols

PDI = polydispersity index

R_{cta} = rate of chain transfer to agent

R_{LCB} = rate of long-chain branching

R_p = rate of chain growth

R_β = rate of β-hydride elimination

X_n = number-average chain length

X_w = weight-average chain length

κ = rate coefficient for polyol chain growth corrected for exchange

$[\eta]$ = intrinsic viscosity

τ = reactor residence time

Literature Cited

(1) Wittcoff, H. A.; Reuben, B. G.; Plotkin, J. S. *Industrial Organic Chemicals*, 2nd Edition; Wiley: Hoboken, NJ, 2004.

(2) *Chem. Eng. News* **2006**, *84* (28), 35. (Facts and Figures of the Chemical Industry, July 10, 2006.)

(3) Villa, C. M.; Dihora, J. O.; Ray, W. H. Effects of Imperfect Mixing on Low-Density Polyethylene Reactor Dynamics. *AIChE J.* **1998**, *44*, 1646.

(4) Chadwick, J. C.; Morini, G.; Balbontin, G.; Camurati, I.; Heere, J. R.; Mingozzi, I.; Testoni, F. Effects of Internal and External Donors on the Regio and Stereoselectivity of Active Species in $MgCl_2$-Supported Catalysts for Propene Polymerization. *Macromol. Chem. Phys.* **2001**, *202*, 1995.

(5) Busico, V.; Cipullo, R.; Corradini, P. Hydrooligomerization of propene: a fingerprint of a Ziegler-Natta catalyst, 1. Preliminary results for $MgCl_2$-supported systems. *Makromol. Chem. Rapid Commun.* **1992**, *13*, 15.

(6) Keii, T. *Kinetics of Ziegler−Natta Polymerization*; Chapman and Hall: London, 1972.

(7) Latado, A.; Embiruc, M.; Mattos., A. G.; Pinto, J. C. Modeling of end-use properties of poly(propylene/ethylene) resins. *Polym. Test.* **2001**, *20*, 419.

(8) Villa, C.; Samson, J. J.; Pierini, P. Model Development in Slurry Processes for Propylene Polymerization. In *8th International Workshop on Polymer Reaction Engineering*; Kreysa, G., Ed.; Wiley−VCH: Weinheim, Germany, 2005.

(9) Balsam, M.; Barghoorn, P.; Stebani, U. Trends in applied macromolecular chemistry. *Angew. Makromol. Chem.* **1999**, *267*, 1.

(10) Hutchinson, R. A.; Ray, W. H. Polymerization of Olefins Through Heterogeneous Catalysts. VIII. Monomer Sorption Effects. *J. Appl. Polym. Sci.* **1990**, *41*, 51.

(11) Guzmán, J. D.; Schieber, J. D.; Pollard, R. A regularization-free method for the calculation of molecular weight distributions from dynamic moduli data. *Rheol. Acta* **2005**, *44*, 342.

(12) Drott, E. E.; Mendelson, R. A. Determination of Polymer Branching with Gel-Permeation Chromatography. I. Theory. *J. Polym. Sci.: Polym. Phys. Ed.* **1970**, *8*, 1361.

(13) Zimm, B. H.; Stockmayer, W. H. The Dimensions of Chain Molecules Containing Branches and Rings. *J. Chem. Phys.* **1949**, *17*, 1301.

(14) Zabisky, R. C. M.; Chan, W. M.; Gloor, P. E.; Hamielec, A. E. A kinetic model for olefin polymerization in high-pressure tubular reactors: a review and update. *Polymer* **1992**, *33*, 2243.

(15) Hutchinson, R. A. Modeling of Chain Length and Long-Chain Branching Distributions in Free-Radical Polymerization. *Macromol. Theory Simul.* **2001**, *10*, 144.

(16) Chum, S. P.; Kruper, W. J.; Guest, M. J. Materials Properties Derived from INSITE Metallocene Catalysts. *Adv. Mater.* **2000**, *12*, 1759.

(17) Soares, J. B. P.; Hamielec, A. E. Bivariate chain length and long chain branching distribution for copolymerization of olefins and polyolefin chains containing terminal double-bonds. *Macromol. Theory Simul.* **1996**, *5*, 547.

(18) Matyjaszewski, K. Macromolecular engineering: From rational design through precise macromolecular synthesis and processing to targeted macroscopic material properties. *Prog. Polym. Sci.* **2005**, *30*, 858.

(19) Penczek, S.; Biela, T.; Duda, A. Living polymerization with reversible chain transfer and reversible deactivation: The case of cyclic esters. *Macromol. Rapid Commun.* **2000**, *21*, 941.

(20) Bradford, E. B.; McKeever, L. D. Block Copolymers, *Prog. Polym. Sci.* **1977**, *2*, 109.

(21) Flory, P. J. Molecular Size Distribution in Ethylene Oxide Polymers. *J. Am. Chem. Soc.* **1940**, *62*, 1561.

(22) Ionescu, M. *Chemistry and Technology of Polyols for Polyurethanes*; Rapra Technology: Shawbury, U.K., 2005.

(23) Gagnon, S. D. Polyethers, Propylene Oxide Polymers. In *Kirk−Othmer Encyclopedia of Chemical Technology*, 5th Edition; Wiley: New York, 2004.

(24) Denbigh, K. G. Continuous reactions. II. The kinetics of steady-state polymerization. *Trans. Faraday Soc.* **1947**, *43*, 648.

(25) Mülhaupt, R. Catalytic Polymerization and Post Polymerization Catalysis Fifty Years after the Discovery of Ziegler's Catalysts. *Macromol. Chem. Phys.* **2003**, *204*, 289.

(26) Le-Khac, B.; Wang, W. Double-metal cyanide catalysts which can be used to prepare polyols and the processes related thereto. U.S. Patent 6,696,383, Feb. 24, 2004.

(27) Pazos, J. F.; Shih, T. T. Continuous preparation of low unsaturation polyoxyalkylene polyether polyols with continuous addition of starter. U.S. Patent 5,689,012, Nov. 18, 1997.

(28) Smith, G. B.; Russell, G. T.; Yin, M.; Heuts, J. P. A. The effects of chain length dependent propagation and termination on the kinetics of free-radical polymerization at low chain lengths. *Eur. Polym. J.* **2005**, *41*, 225.

(29) Radke, W.; Litvinenko, G.; Müller, A. H. E. Effect of Core-Forming Molecules on Molecular Weight Distribution and Degree of Branching in the Synthesis of Hyperbranched Polymers. *Macromolecules* **1998**, *31*, 239.